Published in final edited form as:

Curr Opin Biotechnol. 2016 August ; 40: 193–207. doi:10.1016/j.copbio.2016.03.012.

Extracting Structural and Functional Features of Widely Distributed Biological Circuits with Single Cell Resolution via Tissue Clearing and Delivery Vectors

Jennifer B. Treweek and **Viviana Gradinaru***

Division of Biology and Biological Engineering, California Institute of Technology, Pasadena, CA, USA

Abstract

The scientific community has learned a great deal from imaging small and naturally transparent organisms such as nematodes and zebrafish. The consequences of genetic mutations on their organ development and survival can be visualized easily and with high-throughput at the organism-wide scale. In contrast, three-dimensional information is less accessible in mammalian subjects because the heterogeneity of light-scattering tissue elements renders their organs opaque. Likewise, genetically labeling desired circuits across mammalian bodies is prohibitively slow and costly via the transgenic route. Emerging breakthroughs in viral vector engineering, genome editing tools, and tissue clearing can render larger opaque organisms genetically tractable and transparent for whole-organ cell phenotyping, tract tracing and imaging at depth.

Graphical Abstract

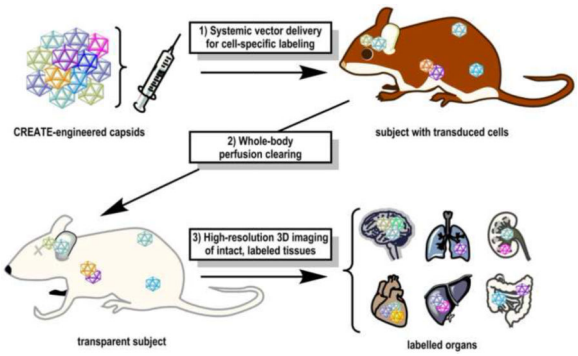

*To whom correspondence should be addressed: Viviana Gradinaru, Ph.D., Division of Biology and Biological Engineering, California Institute of Technology, 1200 East California Blvd MC 156-29, Pasadena, CA 91125, Phone: (626) 395 6813, viviana@caltech.edu.

Competing Interests Statement

California Institute of Technology filed intellectual property for the technologies described with authors as inventors.

Introduction – The case for a hermeneutic approach to biological investigation

From slime mold to the rhesus macaque, countless species have contributed to our current understanding of the biological processes that grant life. The optimum animal model for a line of research is often determined by a particular anatomical feature that makes the organism uniquely suitable for experimentation. For example, although the giant squid may seem an unusual choice to further understanding of mammalian neural circuits, the sheer size and slow conduction velocity of its axons enabled scientists to study neuronal firing with the rudimentary electrophysiological techniques available during the early 20th century [1], giving rise to the field of modern cellular neuroscience. By examining individual aspects of a diverse range of organisms in great detail, scientists have been able to amass a set of unifying principles for the field of neural sciences [2]. The route to this understanding parallels the hermeneutic circle, a classic concept in theology and logic [3]. In hermeneutics, the process of interpretation follows a spiraling path in which one first studies the overall body, then examines its composite parts, and lastly revisits the concept of the whole body as a sum of the parts. Similarly, in neuroscience, observation of a particular sensory or motor system in an organism leads to investigation of the cellular underpinnings of the related circuits, which are then placed in the larger context of the central and peripheral nervous systems.

Applying this approach to investigations of molecular and cellular physiology in health and disease (Table 1, first column) can be both technologically challenging and time-consuming in mammalian subjects. Mammalian tissues can be easily photographed at the macroscopic level, and then the organs and tissues can be dissected and thinly sliced for microscopic analysis. However, the process of aligning these two different perspectives to reconstruct a whole-organism map with subcellular resolution remains nontrivial [4]. Without a clear methodology for integrating microscale and macroscale views, it is difficult to apply newly-discovered molecular mechanisms to systems-level questions and to recognize how systems-level findings may in turn inform novel hypotheses on molecular processes.

Two recent technical advances can bridge the divide between cellular and systems-level studies (Table 1). First, improved viral-vector-based strategies can deliver cargo, such as fluorescent labels, efficiently and with cell specificity over entire organs or the whole body. This enables tracing of, for example, wide-coverage brain networks or peripheral nerves ([5–14], reviews: [15–20]). Second, optimized tissue-clearing methodologies (Table 2–3) can map intact local and long-range circuits [21–41]. The former merges two powerful biological techniques: the use of genetically encoded tools for studying cellular function and connectivity, and the development of viral vectors as a vehicle for delivering these tools into cells [10,11,13,19,42–54]. The latter illustrates how the century-old technique [55,56] of tissue clearing may gain renewed importance when it is refined to incorporate current advances in microscopy [27,29,57–61], genetically encoded fluorescent labeling tools [7,8,14,62–66], protein affinity tags [67–71], and tissue-binding size-adjustable polymeric scaffolding [22,29,32,37,41,72,73]. This brief review will highlight recent work on generating adeno-associated viruses with unique properties via specialized viral-vector

screening methods [53,74–80] (Figure 1, Box 1), and on modern tissue-clearing methodologies that preserve fluorescence and support high-resolution imaging at depth (Figure 2, Table 2, and Box 1; the following protocols generally achieve both goals: [21–25,28,29,31,32,35–37,39–41,81–83] and uDISCO, which outperforms 3DISCO in fluorescence preservation, personal communication with Dr. Ali Ertürk).

Scientific motivation for broad coverage gene delivery and imaging of whole intact tissues in mammals by tissue clearing

Although viral vectors are commonly used for delivering genetically encoded cargo to mammalian cells *in vivo*, therefore avoiding slow and costly transgenic means, few are capable of both safe and efficient transduction of specific cellular targets. Fewer still are capable of broad coverage across all cellular connectivity under study. For example, adeno-associated viruses (AAVs) are widely used, especially in non-dividing cells, due to their safety [78,84–86]; however, the handful of serotypes available cannot efficiently and specifically target many populations of interest. Past and ongoing efforts on engineering viral vectors with desired properties [79,87,88], including cell-type and/or organ specificity [74–77,79,89], will greatly benefit research in mapping and genome editing [90]. To contribute to and complement these efforts we have recently developed an *in vivo C*re-*RE*combination-based *A*AV *T*argeted *E*volution (CREATE) selection platform for identifying AAVs that more efficiently transduce genetically defined cell populations (Figure 1A) [53]. We used CREATE to identify variants from a systemically delivered AAV capsid library that cross the blood–brain barrier and transduce neurons and astrocytes brain-wide. Using this method, we identified one variant, AAV-PHP.B[1], that achieves 40- to 90-fold more efficient brain-wide transduction than the current standard, AAV9 (Figure 1D) [91]. AAV-PHP.B transduces most neuronal types and glia throughout the brain, which supports its use to deliver multicolor labels to genetically defined circuits for mapping distributed networks, such as those recruited by deep brain stimulation [92–97]. Furthermore, engineered vectors that label discrete cell populations could be put to immediate use, for example in elucidating points of contact between major somatic sensory nerves and the CNS, or in mapping the autonomic motor branch of the PNS to better understand metabolic and endocrine disorders.

Despite these new labeling technologies, it remains difficult to create maps for phenotypically distinct fine axons that run in bundles throughout the brain when the traditional method involves sectioning the tissue into paper-thin slices, imaging each slice, and recovering the 3D perspective with imaging software: it is slow, tedious, costly, and error prone. Over the past decade there has been a surge in methods for increasing the transparency of thick mammalian tissue samples and whole organs so that they may be examined intact (Table 2). Here, the scientific value of fluorescence-preserving tissue clearing for vector engineering is also apparent: the ability to process major organs simultaneously and without sectioning (Figure 1B–C) will greatly facilitate transduction

[1]Novel AAV capsid: AAV-PHP.B was named in honor of Caltech Professor Paul H. Patterson (1943–2014).

mapping of systemically delivered genes (Figure 1D), including small-molecule tags and fluorescent labels.

Whole-organ and whole-body tissue-clearing methodologies

The original century-old tissue-clearing techniques [55,56] enable deep imaging into tissue without physical sectioning, but the harsh organic solvents damage cellular architecture and are incompatible with modern immunolabeling and fluorescence microscopy tools. Thus, the application of modern labeling technologies to *ex vivo* mapping studies requires new developments to render tissues transparent while also stabilizing critical macromolecules and preserving endogenous fluorescence (see Table 2 for a comprehensive list of major clearing protocols of the last decade). In particular, the CLARITY technique provides a method to further stabilize samples by anchoring tissue components in place using an interpolating hydrogel scaffold [22,37]. This transparent, tissue-binding hydrogel mesh secures proteins and nucleic acids into place without causing epitope masking and allows scientists to visualize intact organs at the subcellular [40,41] and even single transcript scale [22,29,32,37,41]. Recently, a method to clear whole adult rodents and organs emerged from the realization that hydrogel monomers as well as clearing detergents and immunolabeling reagents could all be infused throughout the intact post-mortem organism using the intrinsic circulatory system (vasculature) (Figure 1B–C, Figure 2A–B) [32,41]; PARS (Perfusion-assisted Agent Release in Situ) achieves delipidation and labeling steps rapidly in the intact post-mortem organism via perfusion. The PARS approach, which has also proven compatible with a variety of tissue-clearing reagents [25,31,39,40], can prepare transparent whole organisms for imaging at depth and aligns with a paradigm shift in biomedical research. Namely, efforts to profile the two-dimensional molecular content of samples have been superseded by more comprehensive inquiries into the relationship between an organ's volumetric composition and its resulting biological function [98].

Across most disciplines and within a variety of laboratory settings, it has become increasingly relevant to engage in the fine-scale phenotyping of whole specimens, whether of intact samples, such as tissue biopsies, excised organs and cultured organs in a dish [99,100], or of whole organisms. Thus, tissue clearing methods must be simple, economical and adaptable to a variety of applications to be adopted across scientific fields. Toward this goal, we developed a set of hydrogel-embedding and delipidation protocols that can be used to rapidly clear excised organs individually or all organs simultaneously within the intact body without compromising cellular architecture or endogenous fluorescence (for experimental timeline and details, see Tables 2–3; for troubleshooting advice, see: http://www.nature.com/nprot/journal/v10/n11/fig_tab/nprot.2015.122_T5.html) [32,41]. PACT (PAssive CLARITY Technique) and PARS entail hybridizing the tissue sample to polymers in order to anchor proteins and nucleic acids during detergent-mediated lipid extraction and to preserve gross tissue architecture during all tissue-processing steps (Figure 1B–C, Figure 2A–B) [32,41]. While many clearing protocols are successful at removing lipids through detergent treatment alone, we have found that the porous structure of the tissue–hydrogel matrix, particularly when coupled to the driving force of detergent perfusion, facilitates rapid diffusion of solubilized lipids out of the tissue and the subsequent penetration of immunolabels into the remaining tissue–hydrogel matrix. Furthermore, the utility of tissue-

hydrogel hybridization and detergent perfusion extends beyond their capacity to facilitate rodent organ and whole-body clearing and immunolabeling [32,41]. For example, hydrogel embedding effectively stabilizes amorphous or fragile samples [41], such as sputum (unpublished results), for processing, and secures microorganisms to sites of infection. This latter property has proven valuable in studying bacterial colonization (personal communication with Dianne Newman). Although originally demonstrated in whole rodents, perfusion-based methods may also render large, excised samples such as primate and pig organs transparent via the recirculation of PARS reagents through catheterized organ vasculature [101], an undertaking which would be prohibitively slow via passive immersion-based clearing. Finally, after initial lipid extraction and/or solvation steps (Table 2, chemical clearing), most tissue-clearing protocols employ a refractive-index homogenization step to minimize differences in light deflection by the heterogeneous tissue biomolecules (Table 3, optical clearing). This is most commonly accomplished via immersing chemically cleared samples in a solution of matched refractive index, such as RIMS (Figure 2A) [32,41]; polyol and concentrated sugar or sugar alcohol solutions such as glycerol [22], sucrose and fructose [21,24,39,102]; or organic solvents such as BABB [27,28,82] and others (see Table 3).

The ability to expediently process and analyze samples without sectioning has revolutionized modern histology. For example, tissue clearing allows pathologists to map tumor cells in whole human biopsies and postmortem samples [41]. Likewise, the ability to conduct fast whole-body clearing, as granted by the perfusive force in the PARS methodology [39], opens new avenues for exploring small-molecule biodistribution, examining viral-vector tropism (Figure 1), and tracing peripheral nerve networks to their target organs (Table 1) [31,32,39,41]. For difficult-to-clear bone samples, PACT with decalcification (PACT-deCAL [41]), SeeDB [103], 3DISCO [28], Murray’s clear (1:2 Benzyl Alcohol: Benzyl Benzoate; BABB [27]) [104] and other decalcification methods [105] all facilitate mapping the three-dimensional architecture of skeletal tissue and stem cell niches [106]. Regardless of the clearing protocol used, all carry trade-offs in terms of the degree of optical transparency achieved, the maintenance of endogenous fluorescence, the preservation of cellular integrity, and the permeability of cleared tissue to macromolecule labels. Although clearing with organic solvents or with electrophoresis may deliver more rapid and effective clearing than passive methods involving immersion in aqueous solutions, these harsher methods may also hinder fluorescent imaging, prove incompatible with immunolabeling, or risk tissue damage (see Table 2). In selecting a specific protocol or shuffling aspects of multiple protocols [107], researchers must consider their project objectives (e.g., imaging sparse epitopes, whole-body tract tracing) and experimental constraints (e.g., integration with smFISH or electron microscopy studies on cleared samples). Thus, this comprehensive list of available protocols (Tables 2–3) will serve most experimental needs (Table 1).

Towards structure–function mapping with tissue clearing

For tissue-clearing methods to reach their full potential, several major challenges must first be tackled: (1) Imaging: large tissue volumes require specialized microscopy; (2) Data analysis: meaningful data must be extracted from terabyte data sets; (3) Access to functional information: markers of activity must be preserved during tissue processing.

Regarding the extraction of functional information, a record of neuronal activity can be encoded via transcriptional or biochemical changes. For example, immediate-early-gene activation (e.g. through *T*argeted *R*ecombination in *A*ctive *P*opulations, or TRAP [108–111]), Ca^{2+} influx, and voltage spikes can all be detected by genetically encoded fluorescing sensors (for reviews, see [112–114]) [53,111,115–118]. An exciting possibility for resolving neuronal activation across longer timescales is to pair this *in vivo* activity sensing with *ex vivo* analysis of previously active cell circuits using thick-tissue clearing. Specifically, genetically encoded stable fluorescent markers can permanently tag living cells that respond to time-restricted stimuli so that their chemical identity and connectivity can be probed post-mortem. One such marker, CaMPARI (calcium-modulated photoactivatable ratiometric integrator of neuronal activity), grants persistent quantitative detection of any neuronal activity that occurs during subsecond application of the photoconversion light [64,119]. One can envision the combined use of CaMPARI with subsequent tissue-clearing methods that preserve endogenous fluorescence (such as Sca*l*eS [40] clearing and RIMS incubation [32,41]) to map the activity of intact biological networks in response to behaviorally relevant stimuli.

As we learn more about the transcriptional correlates of neuronal activity, quantitative and multiplexed RNA detection in intact tissue could also serve the role of extracting functional proxies from deceased tissue. Combinatorial labeling (“barcoding”) via single-molecule fluorescence *in situ* hybridization (smFISH) [120,121] allows for simultaneous detection of mRNA transcripts for multiple genes within individual cells [122,123]. Importantly, smFISH has been validated in thick sections, wherein tissue clearing and swelling improve single-transcript resolution through reducing background and physically separating single-molecule labels [32,122]. Further enlargement of the optical space within a cell, either for fluorescently barcoding multiple transcripts or for examining single-cell morphology, may be achieved through recent protocols (e.g. ExM [72], ePACT [41]) that expand tissue four-fold or more with the possibility to retain endogenous fluorescence (Figure 2C–D for ePACT; [41]). Combined, these evolving technologies raise the possibility of single-cell transcriptomics with preserved spatial information. By applying high-resolution microscopy [58–60,124] to the detection of mRNA-binding probes (e.g., single-molecule hybridization chain reaction (smHCR) probes with high signal-to-noise [125–127]) in cleared and, if needed, expanded tissue, scientists will be able to achieve more robust single-molecule RNA detection and hence quantitative data for transcriptional profiling of intact circuits across organs [122,123,128].

Outlook

Studies in naturally transparent organisms have recently progressed to real-time monitoring of neuronal activity during controlled behavior via light-gated and light-emitting tools [118,129]. Although the protocols for tissue stabilization and lipid removal described above can produce samples with sufficient transparency for intact tissue imaging and rapid tissue phenotyping, these methods are limited to *ex vivo* use. Transparent or not, deceased tissue can offer only a static picture of neuronal connections. Even with a connectome in hand as a road-map for cellular networks, we would still be far from understanding the brain. For example, neuropeptides can act at a distance disregarding explicit wiring [130–132], parallel

pathways within a network can result in degeneracy in circuit function [133], and apparent structural connectivity (e.g. as elucidated via GRASP [134]) does not imply active synaptic connectivity [135]. A crucial next step will involve registering the three-dimensional information obtained through tissue-clearing with either *ex vivo* or *in vivo* cellular activity mapping. Compatible with cleared tissue imaging, methods such as TRAP [108–111] and smFISH [32,122] enable the permanent tagging of recently active cells in thick tissues. This snapshot only captures a single time point, however. What remains to be developed is a method for time-stamping signaling events across bulk cell populations such that the time-varying metabolic information from a single-cell's lifetime can be retrieved and cross-correlated to the metabolic records of all neighboring cells. To this end, single-cell transcriptomics [136,137] and 'molecular ticker tapes' (i.e. an engineered DNA polymerase mis-incorporates nucleotides into a DNA 'ticker tape' based on spikes in ion concentration [138,139]) represent two areas of promise.

A second approach under development aims to bring the CLARITY concept to living tissue. Namely, instead of altering tissue to reduce light-scattering, scientists are recruiting the power of ultrasound focusing at depth to deliver and collect light non-invasively from living tissue. Methods such as Time-Reversal Ultrasound-Encoded (TRUE) aim to correct the light-wavefront in scattering tissue [140] and currently enable focusing at depth within *ex vivo* tissue [141,142]. Because of its high sensitivity to motion, challenges remain in using TRUE for noninvasive deep-tissue imaging and light delivery *in vivo* [143]. One possibility is to combine advances in optical imaging, such as TRUE, with the application of gentle tissue clearing reagents *in vivo* to decrease autofluorescent background and homogenize the refractive index [144,145].

Bringing "clarity" to living tissue, when combined with developments in labeling, imaging, and computation, will enable mapping of anatomical and functional connectivity and will illuminate the workings of intact circuits with high temporal precision. Although whole-body imaging is still a nascent technology, analysis of the resulting volumetric datasets will convey a level of scientific understanding that cannot be replicated in a two-dimensional context; akin to previous work in the nematode and zebrafish, large-scale tissue clearing represents a first step towards a hermeneutic approach to mammalian biology.

Acknowledgments

We thank members of the Long Cai, Viviana Gradinaru, Dianne Newman, and Changhuei Yang groups at Caltech for useful discussions. Dr. Gradinaru is a Heritage Principal Investigator supported by the Heritage Medical Research Institute. This work was funded by grants to VG: the NIH Director's New Innovator IDP20D017782-01 and NIH/NIA 1R01AG047664-01; as well as by funding support from the Beckman Institute for the Resource Center on CLARITY, Optogenetics, and Vector Engineering for technology development and broad dissemination (http://www.beckmaninstitute.caltech.edu/clover.shtml).

References and Recommended Reading

Papers of particular interest, published within the period of review, have been highlighted as:

• of special interest

•• of outstanding interest

1. Hodgkin AL, Huxley AF. Action Potentials Recorded from Inside a Nerve Fibre. Nature. 1939; 144:710–711.
2. Strange K. Revisiting the Krogh Principle in the post-genome era: Caenorhabditis elegans as a model system for integrative physiology research. J Exp Biol. 2007; 210:1622–1631. [PubMed: 17449828]
3. Wikswo JP, Porter AP. Biology coming full circle: Joining the whole and the parts. Exp Biol Med (Maywood). 2015; 240:3–7. [PubMed: 25583953]
4. Bruggeman FJ, Westerhoff HV. The nature of systems biology. Trends Microbiol. 2007; 15:45–50. [PubMed: 17113776]
5. Osakada F, Callaway EM. Design and generation of recombinant rabies virus vectors. Nat Protoc. 2013; 8:1583–1601. [PubMed: 23887178]
6. Schwarz LA, Miyamichi K, Gao XJ, Beier KT, Weissbourd B, DeLoach KE, Ren J, Ibanes S, Malenka RC, Kremer EJ, et al. Viral-genetic tracing of the input-output organization of a central noradrenaline circuit. Nature. 2015; 524:88–92. [PubMed: 26131933]
7. Livet J, Weissman TA, Kang H, Draft RW, Lu J, Bennis RA, Sanes JR, Lichtman JW. Transgenic strategies for combinatorial expression of fluorescent proteins in the nervous system. Nature. 2007; 450:56–62. [PubMed: 17972876]
8. Tsuriel S, Gudes S, Draft RW, Binshtok AM, Lichtman JW. Multispectral labeling technique to map many neighboring axonal projections in the same tissue. Nat Methods. 2015; 12:547–552. [PubMed: 25915122] ••A “GPS” for the brain. From the lab that brought brainbow comes a technique for mapping the location of axonal branches of many individual neurons simultaneously and at the resolution of individual axons.
9. Salinas S, Bilsland LG, Henaff D, Weston AE, Keriel A, Schiavo G, Kremer EJ. CAR-Associated Vesicular Transport of an Adenovirus in Motor Neuron Axons. PLoS Pathog. 2009; 5:e1000442. [PubMed: 19461877]
10. Cetin A, Callaway EM. Optical control of retrogradely infected neurons using drug-regulated "TLoop" lentiviral vectors. J Neurophysiol. 2014; 111:2150–2159. [PubMed: 24572099]
11. Wall NR, Wickersham IR, Cetin A, De La Parra M, Callaway EM. Monosynaptic circuit tracing in vivo through Cre-dependent targeting and complementation of modified rabies virus. Proc Natl Acad Sci U S A. 2010; 107:21848–21853. [PubMed: 21115815]
12. Marshel JH, Mori T, Nielsen KJ, Callaway EM. Targeting single neuronal networks for gene expression and cell labeling in vivo. Neuron. 2010; 67:562–574. [PubMed: 20797534]
13. Osakada F, Mori T, Cetin AH, Marshel JH, Virgen B, Callaway EM. New rabies virus variants for monitoring and manipulating activity and gene expression in defined neural circuits. Neuron. 2011; 71:617–631. [PubMed: 21867879]
14. Fenno LE, Mattis J, Ramakrishnan C, Hyun M, Lee SY, He M, Tucciarone J, Selimbeyoglu A, Berndt A, Grosenick L, et al. Targeting cells with single vectors using multiple-feature Boolean logic. Nat Methods. 2014; 11:763–772. [PubMed: 24908100] ••The INTRSECT (INTronic Recombinase Sites Enabling Combinatorial Targeting) strategy grants the conditional labeling of discrete neuronal populations and circuits using viral vectors with specialized trafficking properties and taking advantage of available recombinase tools. Importantly, INTRSECT can replicate numerous Boolean logical operations within the same subject, allowing researchers to control multiple genetically and/or connectivity-defined pathways.
15. Ekstrand MI, Enquist LW, Pomeranz LE. The alpha-herpesviruses: molecular pathfinders in nervous system circuits. Trends Mol Med. 2008; 14:134–140. [PubMed: 18280208]
16. Callaway EM. Transneuronal circuit tracing with neurotropic viruses. Curr Opin Neurobiol. 2008; 18:617–623. [PubMed: 19349161]
17. Song CK, Enquist LW, Bartness TJ. New developments in tracing neural circuits with herpesviruses. Virus Res. 2005; 111:235–249. [PubMed: 15893400]
18. Ugolini G. Advances in viral transneuronal tracing. J Neurosci Methods. 2010; 194:2–20. [PubMed: 20004688]
19. Nassi JJ, Cepko CL, Born RT, Beier KT. Neuroanatomy goes viral! Front Neuroanat. 2015; 9:80. [PubMed: 26190977]

20. Saunders, A.; Sabatini, BL. Curr Protoc Neurosci. John Wiley & Sons, Inc; 2001. Cre Activated and Inactivated Recombinant Adeno-Associated Viral Vectors for Neuronal Anatomical Tracing or Activity Manipulation.
21. Ke M-T, Fujimoto S, Imai T. SeeDB: a simple and morphology-preserving optical clearing agent for neuronal circuit reconstruction. Nat Neurosci. 2013; 16:1154–1161. [PubMed: 23792946]
22. Chung K, Wallace J, Kim SY, Kalyanasundaram S, Andalman AS, Davidson TJ, Mirzabekov JJ, Zalocusky KA, Mattis J, Denisin AK, et al. Structural and molecular interrogation of intact biological systems. Nature. 2013; 497:332–337. [PubMed: 23575631]
23. Hama H, Kurokawa H, Kawano H, Ando R, Shimogori T, Noda H, Fukami K, Sakaue-Sawano A, Miyawaki A. Scale: a chemical approach for fluorescence imaging and reconstruction of transparent mouse brain. Nat Neurosci. 2011; 14:1481–1488. [PubMed: 21878933]
24. Kuwajima T, Sitko AA, Bhansali P, Jurgens C, Guido W, Mason C. ClearT: a detergent-and solvent-free clearing method for neuronal and non-neuronal tissue. Development. 2013; 140:1364–1368. [PubMed: 23444362]
25. Susaki EA, Tainaka K, Perrin D, Kishino F, Tawara T, Watanabe TM, Yokoyama C, Onoe H, Eguchi M, Yamaguchi S, et al. Whole-brain imaging with single-cell resolution using chemical cocktails and computational analysis. Cell. 2014; 157:726–739. [PubMed: 24746791]
26. Becker K, Jährling N, Saghafi S, Weiler R, Dodt H-U. Chemical clearing and dehydration of GFP expressing mouse brains. PLoS One. 2012; 7:e33916. [PubMed: 22479475]
27. Dodt H-U, Leischner U, Schierloh A, Jährling N, Mauch CP, Deininger K, Deussing JM, Eder M, Zieglgänsberger W, Becker K. Ultramicroscopy: three-dimensional visualization of neuronal networks in the whole mouse brain. Nat Methods. 2007; 4:331–336. [PubMed: 17384643]
28. Ertürk A, Becker K, Jahrling N, Mauch CP, Hojer CD, Egen JG, Hellal F, Bradke F, Sheng M, Dodt HU. Three-dimensional imaging of solvent-cleared organs using 3DISCO. Nat Protoc. 2012; 7:1983–1995. [PubMed: 23060243]
29. Tomer R, Ye L, Hsueh B, Deisseroth K. Advanced CLARITY for rapid and high-resolution imaging of intact tissues. Nat Protoc. 2014; 9:1682–1697. [PubMed: 24945384]
30. Zhang MD, Tortoriello G, Hsueh B, Tomer R, Ye L, Mitsios N, Borgius L, Grant G, Kiehn O, Watanabe M, et al. Neuronal calcium-binding proteins 1/2 localize to dorsal root ganglia and excitatory spinal neurons and are regulated by nerve injury. Proc Natl Acad Sci U S A. 2014; 111:E1149–E1158. [PubMed: 24616509]
31. Hou B, Zhang D, Zhao S, Wei M, Yang Z, Wang S, Wang J, Zhang X, Liu B, Fan L, et al. Scalable and DiI-compatible optical clearance of the mammalian brain. Front Neuroanat. 2015; 9:19. [PubMed: 25759641]
32. Yang B, Treweek JB, Kulkarni RP, Deverman BE, Chen CK, Lubeck E, Shah S, Cai L, Gradinaru V. Single-cell phenotyping within transparent intact tissue through whole-body clearing. Cell. 2014; 158:945–958. [PubMed: 25088144]
33. Sakhalkar HS, Dewhirst M, Oliver T, Cao Y, Oldham M. Functional imaging in bulk tissue specimens using optical emission tomography: fluorescence preservation during optical clearing. Phys Med Biol. 2007; 52:2035–2054. [PubMed: 17404454]
34. Aoyagi Y, Kawakami R, Osanai H, Hibi T, Nemoto T. A rapid optical clearing protocol using 2,2'-thiodiethanol for microscopic observation of fixed mouse brain. PLoS One. 2015; 10:e0116280. [PubMed: 25633541]
35. Tainaka K, Kubota SI, Suyama TQ, Susaki EA, Perrin D, Ukai-Tadenuma M, Ukai H, Ueda HR. Whole-body imaging with single-cell resolution by tissue decolorization. Cell. 2014; 159:911–924. [PubMed: 25417165]
36. Renier N, Wu Z, Simon DJ, Yang J, Ariel P, Tessier-Lavigne M. iDISCO: a simple, rapid method to immunolabel large tissue samples for volume imaging. Cell. 2014; 159:896–910. [PubMed: 25417164]
37. Chung K, Deisseroth K. CLARITY for mapping the nervous system. Nat Methods. 2013; 10:508–513. [PubMed: 23722210]
38. Ertürk A, Bradke F. High-resolution imaging of entire organs by 3-dimensional imaging of solvent cleared organs (3DISCO). Exp Neurol. 2013; 242:57–64. [PubMed: 23124097]

39. Susaki EA, Tainaka K, Perrin D, Yukinaga H, Kuno A, Ueda HR. Advanced CUBIC protocols for whole-brain and whole-body clearing and imaging. Nat Protoc. 2015; 10:1709–1727. [PubMed: 26448360] •A comprehensive description of the CUBIC methods (orignal CUBIC and CUBIC with decolorization), including updates to the reagent list and step-by-step protocols for CUBIC tissue clearing variations and subsequent CUBIC informatics.

40. Hama H, Hioki H, Namiki K, Hoshida T, Kurokawa H, Ishidate F, Kaneko T, Akagi T, Saito T, Saido T, et al. ScaleS: an optical clearing palette for biological imaging. Nat Neurosci. 2015; 18:1518–1529. [PubMed: 26368944] ••A paper that describes multiple notable improvements to the previously reported ScaleA2 method - a clearing protocol that, while gentle on tissues, was slow, immunolabeling-limited, and unable to deliver complete transparency in large samples. ScaleS addresses many of these original limitations with case-specific methods for: rapid clearing, immunostaining and clearing, large-organ clearing, etc.

41. Treweek JB, Chan KY, Flytzanis NC, Yang B, Deverman BE, Greenbaum A, Lignell A, Xiao C, Cai L, Ladinsky MS, et al. Whole-body tissue stabilization and selective extractions via tissue-hydrogel hybrids for high-resolution intact circuit mapping and phenotyping. Nat Protoc. 2015; 10:1860–1896. [PubMed: 26492141] ••Detailed, step-wise instructions for conducting the PACT, PARS, and RIMS methodologies, as well as for imaging large, cleared tissues with an affordable, custom-built light-sheet microscope, and finally for manipulating and analyzing large image data files in commercial and open-source software packages. In addition, this Nature Protocol article describes important updates to the clearing techniques in Yang et al., 2014, including designated procedures for PACT-based expansion-clearing, for PACT-based bone-clearing via a decalcification step, and for the integration of PACT with standard histological methods for quenching autofluorescence.

42. Luo L, Callaway EM, Svoboda K. Genetic dissection of neural circuits. Neuron. 2008; 57:634–660. [PubMed: 18341986]

43. Braz JM, Rico B, Basbaum AI. Transneuronal tracing of diverse CNS circuits by Cre-mediated induction of wheat germ agglutinin in transgenic mice. Proc Natl Acad Sci U S A. 2002; 99:15148–15153. [PubMed: 12391304]

44. Horowitz LF, Montmayeur JP, Echelard Y, Buck LB. A genetic approach to trace neural circuits. Proc Natl Acad Sci U S A. 1999; 96:3194–3199. [PubMed: 10077660]

45. Zampieri N, Jessell TM, Murray AJ. Mapping sensory circuits by anterograde trans-synaptic transfer of recombinant rabies virus. Neuron. 2014; 81:766–778. [PubMed: 24486087]

46. Lo L, Anderson DJ. A Cre-dependent, anterograde transsynaptic viral tracer for mapping output pathways of genetically marked neurons. Neuron. 2011; 72:938–950. [PubMed: 22196330]

47. Mundell NA, Beier KT, Pan YA, Lapan SW, Goz Ayturk D, Berezovskii VK, Wark AR, Drokhlyansky E, Bielecki J, Born RT, et al. Vesicular stomatitis virus enables gene transfer and transsynaptic tracing in a wide range of organisms. J Comp Neurol. 2015; 523:1639–1663. [PubMed: 25688551]

48. Wickersham IR, Lyon DC, Barnard RJ, Mori T, Finke S, Conzelmann KK, Young JA, Callaway EM. Monosynaptic restriction of transsynaptic tracing from single, genetically targeted neurons. Neuron. 2007; 53:639–647. [PubMed: 17329205]

49. Wickersham IR, Finke S, Conzelmann KK, Callaway EM. Retrograde neuronal tracing with a deletion-mutant rabies virus. Nat Methods. 2007; 4:47–49. [PubMed: 17179932]

50. Zhang F, Gradinaru V, Adamantidis AR, Durand R, Airan RD, de Lecea L, Deisseroth K. Optogenetic interrogation of neural circuits: technology for probing mammalian brain structures. Nat Protoc. 2010; 5:439–456. [PubMed: 20203662]

51. Atasoy D, Aponte Y, Su HH, Sternson SM. A FLEX switch targets Channelrhodopsin-2 to multiple cell types for imaging and long-range circuit mapping. J Neurosci. 2008; 28:7025–7030. [PubMed: 18614669]

52. Saunders A, Johnson CA, Sabatini BL. Novel recombinant adeno-associated viruses for Cre activated and inactivated transgene expression in neurons. Front Neural Circuits. 2012; 6:47. [PubMed: 22866029]

53. Deverman BE, Pravdo PL, Simpson BP, Kumar SR, Chan KY, Banerjee A, Wu WL, Yang B, Huber N, Pasca SP, et al. Cre-dependent selection yields AAV variants for widespread gene transfer to the adult brain. Nat Biotechnol. 2016; 34:204–209. [PubMed: 26829320] ••Introduces a

novel selection platform for identifying adeno-associated viruses (AAVs) that can be delivered systemically and more efficiently transduce genetically defined cell populations. The methodology (CREATE) eliminates the need for lengthy selection steps traditionally used in panning capsid libraries. As proof-of-principle of the CREATE platform, the isolation of an engineered AAV variant capable of crossing the blood-brain barrier and conferring efficient CNS transduction is described.

54. Sun Y, Nguyen AQ, Nguyen JP, Le L, Saur D, Choi J, Callaway EM, Xu X. Cell-type-specific circuit connectivity of hippocampal CA1 revealed through Cre-dependent rabies tracing. Cell Rep. 2014; 7:269–280. [PubMed: 24656815]
55. Spalteholz, W. Uber das Durchsichtigmachen von menschlichen und tierischen Präparaten und seine theoretischen Bedingungen, nebst Anhang: Uber Knochenfärbung. Leipzig: S. Hirzel; 1914.
56. Spalteholz, W. Handatlas der Anatomie des Menschen. Vol. 2. Leipzig: Hirzel; 1898. p. 2
57. Huisken J, Stainier DYR. Selective plane illumination microscopy techniques in developmental biology. Development. 2009; 136:1963–1975. [PubMed: 19465594]
58. Hess ST, Girirajan TP, Mason MD. Ultra-high resolution imaging by fluorescence photoactivation localization microscopy. Biophys J. 2006; 91:4258–4272. [PubMed: 16980368]
59. Betzig E, Patterson GH, Sougrat R, Lindwasser OW, Olenych S, Bonifacino JS, Davidson MW, Lippincott-Schwartz J, Hess HF. Imaging intracellular fluorescent proteins at nanometer resolution. Science. 2006; 313:1642–1645. [PubMed: 16902090]
60. Rust MJ, Bates M, Zhuang X. Sub-diffraction-limit imaging by stochastic optical reconstruction microscopy (STORM). Nat Methods. 2006; 3:793–796. [PubMed: 16896339]
61. Hell SW, Wichmann J. Breaking the diffraction resolution limit by stimulated emission: stimulated-emission-depletion fluorescence microscopy. Opt Lett. 1994; 19:780–782. [PubMed: 19844443]
62. Chen TW, Wardill TJ, Sun Y, Pulver SR, Renninger SL, Baohan A, Schreiter ER, Kerr RA, Orger MB, Jayaraman V, et al. Ultrasensitive fluorescent proteins for imaging neuronal activity. Nature. 2013; 499:295. [PubMed: 23868258]
63. Akerboom J, Chen TW, Wardill TJ, Tian L, Marvin JS, Mutlu S, Calderon NC, Esposti F, Borghuis BG, Sun XR, et al. Optimization of a GCaMP Calcium Indicator for Neural Activity Imaging. J Neurosci. 2012; 32:13819–13840. [PubMed: 23035093]
64. Fosque BF, Sun Y, Dana H, Yang C-T, Ohyama T, Tadross MR, Patel R, Zlatic M, Kim DS, Ahrens MB, et al. Labeling of active neural circuits in vivo with designed calcium integrators. Science. 2015; 347:755–760. [PubMed: 25678659] ••Report of a neuronal activity sensor - CaMPARI, based on Ca^{2+}-binding protein calmodulin (CaM) and the photoconvertible fluorescent protein mEos2, that switches from its green-fluorescing to red fluorescing state only when it is simultaneously illuminated with violet light and exposed to spiking calcium levels.
65. Venkatachalam V, Brinks D, Maclaurin D, Hochbaum D, Kralj J, Cohen AE. Flash Memory: Photochemical Imprinting of Neuronal Action Potentials onto a Microbial Rhodopsin. J Am Chem Soc. 2014; 136:2529–2537. [PubMed: 24428326]
66. Gradinaru V, Zhang F, Ramakrishnan C, Mattis J, Prakash R, Diester I, Goshen I, Thompson KR, Deisseroth K. Molecular and Cellular Approaches for Diversifying and Extending Optogenetics. Cell. 2010; 141:154–165. [PubMed: 20303157]
67. Keppler A, Gendreizig S, Gronemeyer T, Pick H, Vogel H, Johnsson K. A general method for the covalent labeling of fusion proteins with small molecules in vivo. Nat Biotechnol. 2003; 21:86–89. [PubMed: 12469133]
68. Los GV, Encell LP, McDougall MG, Hartzell DD, Karassina N, Zimprich C, Wood MG, Learish R, Ohane RF, Urh M, et al. HatoTag: A novel protein labeling technology for cell imaging and protein analysis. ACS Chem Biol. 2008; 3:373–382. [PubMed: 18533659]
69. Gautier A, Juillerat A, Heinis C, Correa IR, Kindermann M, Beaufils F, Johnsson K. An engineered protein tag for multiprotein labeling in living cells. Chem Biol. 2008; 15:128–136. [PubMed: 18291317]
70. Miller LW, Cai YF, Sheetz MP, Cornish VW. In vivo protein labeling with trimethoprim conjugates: a flexible chemical tag. Nat Methods. 2005; 2:255–257. [PubMed: 15782216]

71. Bedbrook CN, Kato M, Ravindra Kumar S, Lakshmanan A, Nath RD, Sun F, Sternberg PW, Arnold FH, Gradinaru V. Genetically Encoded Spy Peptide Fusion System to Detect Plasma Membrane-Localized Proteins In Vivo. Chem Biol. 2015; 22:1108–1121. [PubMed: 26211362]
72. Chen F, Tillberg PW, Boyden ES. Expansion microscopy. Science. 2015
73. Osten P, Margrie TW. Mapping brain circuitry with a light microscope. Nat Methods. 2013; 10:515–523. [PubMed: 23722211]
74. Grimm D, Lee JS, Wang L, Desai T, Akache B, Storm TA, Kay MA. In vitro and in vivo gene therapy vector evolution via multispecies interbreeding and retargeting of adeno-associated viruses. J Virol. 2008; 82:5887–5911. [PubMed: 18400866]
75. Dalkara D, Byrne LC, Klimczak RR, Visel M, Yin L, Merigan WH, Flannery JG, Schaffer DV. In vivo-directed evolution of a new adeno-associated virus for therapeutic outer retinal gene delivery from the vitreous. Sci Transl Med. 2013; 5:189ra176.
76. Lisowski L, Dane AP, Chu K, Zhang Y, Cunningham SC, Wilson EM, Nygaard S, Grompe M, Alexander IE, Kay MA. Selection and evaluation of clinically relevant AAV variants in a xenograft liver model. Nature. 2014; 506:382–386. [PubMed: 24390344]
77. Maheshri N, Koerber JT, Kaspar BK, Schaffer DV. Directed evolution of adeno-associated virus yields enhanced gene delivery vectors. Nat Biotechnol. 2006; 24:198–204. [PubMed: 16429148]
78. Kaplitt MG, Feigin A, Tang C, Fitzsimons HL, Mattis P, Lawlor PA, Bland RJ, Young D, Strybing K, Eidelberg D, et al. Safety and tolerability of gene therapy with an adeno-associated virus (AAV) borne GAD gene for Parkinson's disease: an open label, phase I trial. Lancet. 2007; 369:2097–2105. [PubMed: 17586305]
79. Mueller C, Ratner D, Zhong L, Esteves-Sena M, Gao G. Production and discovery of novel recombinant adeno-associated viral vectors. Curr Protoc Microbiol. 2012; Chapter 14 Unit14D 11.
80. Gao G, Zhong L, Danos O. Exploiting natural diversity of AAV for the design of vectors with novel properties. Methods Mol Biol. 2011; 807:93–118. [PubMed: 22034027]
81. Kim S-Y, Cho JH, Murray E, Bakh N, Choi H, Ohn K, Ruelas L, Hubbert A, McCue M, Vassallo SL, et al. Stochastic electrotransport selectively enhances the transport of highly electromobile molecules. Proc Natl Acad Sci U S A. 2015
82. Ertürk A, Mauch CP, Hellal F, Forstner F, Keck T, Becker K, Jahrling N, Steffens H, Richter M, Hubener M, et al. Three-dimensional imaging of the unsectioned adult spinal cord to assess axon regeneration and glial responses after injury. Nat Med. 2012; 18:166–171. [PubMed: 22198277]
83. Staudt T, Lang MC, Medda R, Engelhardt J, Hell SW. 2,2'-thiodiethanol: a new water soluble mounting medium for high resolution optical microscopy. Microsc Res Tech. 2007; 70:1–9. [PubMed: 17131355]
84. Maguire AM, Simonelli F, Pierce EA, Pugh EN Jr, Mingozzi F, Bennicelli J, Banfi S, Marshall KA, Testa F, Surace EM, et al. Safety and efficacy of gene transfer for Leber's congenital amaurosis. N Engl J Med. 2008; 358:2240–2248. [PubMed: 18441370]
85. Nathwani AC, Rosales C, McIntosh J, Rastegarlari G, Nathwani D, Raj D, Nawathe S, Waddington SN, Bronson R, Jackson S, et al. Long-term safety and efficacy following systemic administration of a self-complementary AAV vector encoding human FIX pseudotyped with serotype 5 and 8 capsid proteins. Mol Ther. 2011; 19:876–885. [PubMed: 21245849]
86. Gaudet D, de Wal J, Tremblay K, Dery S, van Deventer S, Freidig A, Brisson D, Methot J. Review of the clinical development of alipogene tiparvovec gene therapy for lipoprotein lipase deficiency. Atheroscler Suppl. 2010; 11:55–60. [PubMed: 20427244]
87. Bowles DE, Rabinowitz JE, Samulski RJ. Marker rescue of adeno-associated virus (AAV) capsid mutants: a novel approach for chimeric AAV production. J Virol. 2003; 77:423–432. [PubMed: 12477847]
88. Reardon Thomas R, Murray Andrew J, Turi Gergely F, Wirblich C, Croce Katherine R, Schnell Matthias J, Jessell Thomas M, Losonczy A. Rabies Virus CVS-N2cΔG Strain Enhances Retrograde Synaptic Transfer and Neuronal Viability. Neuron. 2016; 89:711–724. [PubMed: 26804990]
89. Pulicherla N, Shen S, Yadav S, Debbink K, Govindasamy L, Agbandje-McKenna M, Asokan A. Engineering liver-detargeted AAV9 vectors for cardiac and musculoskeletal gene transfer. Mol Ther. 2011; 19:1070–1078. [PubMed: 21364538]

90. Vandenberghe LH, Wilson JM, Gao G. Tailoring the AAV vector capsid for gene therapy. Gene Ther. 2009; 16:311–319. [PubMed: 19052631]
91. Foust KD, Nurre E, Montgomery CL, Hernandez A, Chan CM, Kaspar BK. Intravascular AAV9 preferentially targets neonatal neurons and adult astrocytes. Nat Biotechnol. 2009; 27:59–65. [PubMed: 19098898]
92. Gradinaru V, Mogri M, Thompson KR, Henderson JM, Deisseroth K. Optical Deconstruction of Parkinsonian Neural Circuitry. Science. 2009; 324:354–359. [PubMed: 19299587]
93. Deniau JM, Degos B, Bosch C, Maurice N. Deep brain stimulation mechanisms: beyond the concept of local functional inhibition. Eur J Neurosci. 2010; 32:1080–1091. [PubMed: 21039947]
94. Carron R, Chaillet A, Filipchuk A, Pasillas-Lepine W, Hammond C. Closing the loop of deep brain stimulation. Front Syst Neurosci. 2013; 7
95. Santaniello S, McCarthy MM, Montgomery EB Jr, Gale JT, Kopell N, Sarma SV. Therapeutic mechanisms of high-frequency stimulation in Parkinson's disease and neural restoration via loop-based reinforcement. Proc Natl Acad Sci U S A. 2015; 112:E586–E595. [PubMed: 25624501]
96. Kang G, Lowery MM. Effects of antidromic and orthodromic activation of STN afferent axons during DBS in Parkinson's disease: a simulation study. Front Comput Neurosci. 2014; 8:32. [PubMed: 24678296]
97. Creed M, Pascoli VJ, Lüscher C. Refining deep brain stimulation to emulate optogenetic treatment of synaptic pathology. Science. 2015; 347:659–664. [PubMed: 25657248]
98. Richardson Douglas S, Lichtman Jeff W. Clarifying Tissue Clearing. Cell. 2015; 162:246–257. [PubMed: 26186186] •A solid review on the fundamentals of light interactions with biological matter and the tissue clearing field.
99. Lancaster MA, Knoblich JA. Organogenesis in a dish: modeling development and disease using organoid technologies. Science. 2014; 345:1247125. [PubMed: 25035496]
100. Pasca AM, Sloan SA, Clarke LE, Tian Y, Makinson CD, Huber N, Kim CH, Park JY, O'Rourke NA, Nguyen KD, et al. Functional cortical neurons and astrocytes from human pluripotent stem cells in 3D culture. Nat Methods. 2015; 12:671–678. [PubMed: 26005811]
101. Guyette JP, Gilpin SE, Charest JM, Tapias LF, Ren X, Ott HC. Perfusion decellularization of whole organs. Nat Protoc. 2014; 9:1451–1468. [PubMed: 24874812]
102. Ke MT, Imai T. Optical clearing of fixed brain samples using SeeDB. Curr Protoc Neurosci. 2014; 66 Unit 2.22.
103. Calve S, Ready A, Huppenbauer C, Main R, Neu CP. Optical Clearing in Dense Connective Tissues to Visualize Cellular Connectivity In Situ. PLoS ONE. 2015; 10:e0116662. [PubMed: 25581165]
104. Becker K, Jahrling N, Saghafi S, Dodt HU. Immunostaining, dehydration, and clearing of mouse embryos for ultramicroscopy Cold Spring Harb. Protoc. 2013; 2013:743–744.
105. Kusumbe AP, Ramasamy SK, Starsichova A, Adams RH. Sample preparation for high-resolution 3D confocal imaging of mouse skeletal tissue. Nat Protoc. 2015; 10:1904–1914. [PubMed: 26513669]
106. Acar M, Kocherlakota KS, Murphy MM, Peyer JG, Oguro H, Inra CN, Jaiyeola C, Zhao Z, Luby-Phelps K, Morrison SJ. Deep imaging of bone marrow shows non-dividing stem cells are mainly perisinusoidal. Nature. 2015; 526:126–130. [PubMed: 26416744]
107. Susaki EA, Ueda HR. Whole-body and Whole-Organ Clearing and Imaging Techniques with Single-Cell Resolution: Toward Organism-Level Systems Biology in Mammals. Cell Chem Biol. 2016; 23:137–157. [PubMed: 26933741]
108. Guenthner CJ, Miyamichi K, Yang HH, Heller HC, Luo LQ. Permanent Genetic Access to Transiently Active Neurons via TRAP: Targeted Recombination in Active Populations. Neuron. 2013; 78:773–784. [PubMed: 23764283]
109. Reardon S. Transparent brains reveal effects of cocaine and fear. Nature News. 2014
110. Epp JR, Niibori Y, Hsiang H-L, Mercaldo V, Deisseroth K, Josselyn SA, Frankland PW. Optimization of CLARITY for clearing whole-brain and other intact organs. eneuro. 2015; 2
111. Ye L, Tomer R, Hsueh B, Guenthner CJ, Luo L, Deisseroth K. CLARITY-based whole brain activity mapping with immediate early gene TRAP. Poster abstract at Society for Neuroscience. 2014

112. Gradinaru V, Flytzanis NC. Neuroscience: Fluorescent boost for voltage sensors. Nature. 2016; 529:469–470. [PubMed: 26819038]
113. Knopfel T. Genetically encoded optical indicators for the analysis of neuronal circuits. Nat Rev Neurosci. 2012; 13:687–700. [PubMed: 22931891]
114. Akerboom J, Carreras Calderon N, Tian L, Wabnig S, Prigge M, Tolo J, Gordus A, Orger MB, Severi KE, Macklin JJ, et al. Genetically encoded calcium indicators for multi-color neural activity imaging and combination with optogenetics. Front Mol Neurosci. 2013; 6:2. [PubMed: 23459413]
115. Zoukos Y, Leonard JP, Thomaides T, Thompson AJ, Cuzner ML. beta-Adrenergic receptor density and function of peripheral blood mononuclear cells are increased in multiple sclerosis: a regulatory role for cortisol and interleukin-1. Ann Neurol. 1992; 31:657–662. [PubMed: 1325138]
116. Reardon S. Transparent brains reveal effects of cocaine and fear. Nature. 2014
117. Crosetto N, Bienko M, van Oudenaarden A. Spatially resolved transcriptomics and beyond. Nat Rev Genet. 2015; 16:57–66. [PubMed: 25446315]
118. Flytzanis NC, Bedbrook CN, Chiu H, Engqvist MKM, Xiao C, Chan KY, Sternberg PW, Arnold FH, Gradinaru V. Archaerhodopsin variants with enhanced voltage-sensitive fluorescence in mammalian and Caenorhabditis elegans neurons. Nat Commun. 2014:5.
119. Schreiter, ER.; Fosque, BF.; Sun, Y.; Dana, H.; Ohyama, T.; Yang, C.; Ahrens, MB.; Koyama, M.; Svoboda, K.; Zlatic, M., et al. Society For Neuroscience Annual Meeting. Washington, DC: 2014. Permanent in vivo marking of active neurons with a genetically encoded calcium integrator, CaMPARI.
120. Femino AM, Fay FS, Fogarty K, Singer RH. Visualization of Single RNA Transcripts in Situ. Science. 1998; 280:585–590. [PubMed: 9554849]
121. Raj A, van den Bogaard P, Rifkin SA, van Oudenaarden A, Tyagi S. Imaging individual mRNA molecules using multiple singly labeled probes. Nat Methods. 2008; 5:877–879. [PubMed: 18806792]
122. Lubeck E, Cai L. Single-cell systems biology by super-resolution imaging and combinatorial labeling. Nat Methods. 2012; 9:743–748. [PubMed: 22660740]
123. Lubeck E, Coskun AF, Zhiyentayev T, Ahmad M, Cai L. Single-cell in situ RNA profiling by sequential hybridization. Nat Methods. 2014; 11:360–361. [PubMed: 24681720]
124. Hell SW. Far-field optical nanoscopy. Science. 2007; 316:1153–1158. [PubMed: 17525330]
125. Choi HMT, Beck VA, Pierce NA. Next-Generation in Situ Hybridization Chain Reaction: Higher Gain, Lower Cost, Greater Durability. ACS Nano. 2014; 8:4284–4294. [PubMed: 24712299]
126. Dirks RM, Pierce NA. Triggered amplification by hybridization chain reaction. Proc Natl Acad Sci U S A. 2004; 101:15275–15278. [PubMed: 15492210]
127. Choi HM, Chang JY, Trinh le A, Padilla JE, Fraser SE, Pierce NA. Programmable in situ amplification for multiplexed imaging of mRNA expression. Nat Biotechnol. 2010; 28:1208–1212. [PubMed: 21037591]
128. Sylwestrak Emily L, Rajasethupathy P, Wright Matthew A, Jaffe A, Deisseroth K. Multiplexed Intact-Tissue Transcriptional Analysis at Cellular Resolution. Cell. 2016; 164:792–804. [PubMed: 26871636]
129. Zhang F, Wang LP, Brauner M, Liewald JF, Kay K, Watzke N, Wood PG, Bamberg E, Nagel G, Gottschalk A, et al. Multimodal fast optical interrogation of neural circuitry. Nature. 2007; 446:633–U634. [PubMed: 17410168]
130. Dickinson PS, Mecsas C, Marder E. Neuropeptide fusion of two motor-pattern generator circuits. Nature. 1990; 344:155–158. [PubMed: 2308633]
131. van den Pol AN. Neuropeptide transmission in brain circuits. Neuron. 2012; 76:98–115. [PubMed: 23040809]
132. Flavell SW, Pokala N, Macosko EZ, Albrecht DR, Larsch J, Bargmann CI. Serotonin and the neuropeptide PDF initiate, extend opposing behavioral states in C. elegans. Cell. 2013; 154:1023–1035. [PubMed: 23972393]

133. Gutierrez GJ, O'Leary T, Marder E. Multiple mechanisms switch an electrically coupled, synaptically inhibited neuron between competing rhythmic oscillators. Neuron. 2013; 77:845–858. [PubMed: 23473315]

134. Feinberg EH, Vanhoven MK, Bendesky A, Wang G, Fetter RD, Shen K, Bargmann CI. GFP Reconstitution Across Synaptic Partners (GRASP) defines cell contacts and synapses in living nervous systems. Neuron. 2008; 57:353–363. [PubMed: 18255029]

135. Marder E, Goeritz ML, Otopalik AG. Robust circuit rhythms in small circuits arise from variable circuit components and mechanisms. Curr Opin Neurobiol. 2015; 31:156–163. [PubMed: 25460072]

136. Klein Allon M, Mazutis L, Akartuna I, Tallapragada N, Veres A, Li V, Peshkin L, Weitz David A, Kirschner Marc W. Droplet Barcoding for Single-Cell Transcriptomics Applied to Embryonic Stem Cells. Cell. 2015; 161:1187–1201. [PubMed: 26000487]

137. Macosko Evan Z, Basu A, Satija R, Nemesh J, Shekhar K, Goldman M, Tirosh I, Bialas Allison R, Kamitaki N, Martersteck Emily M, et al. Highly Parallel Genome-wide Expression Profiling of Individual Cells Using Nanoliter Droplets. Cell. 2015; 161:1202–1214. [PubMed: 26000488]

138. Glaser JI, Zamft BM, Marblestone AH, Moffitt JR, Tyo K, Boyden ES, Church G, Kording KP. Statistical analysis of molecular signal recording. PLoS Comput Biol. 2013; 9:e1003145. [PubMed: 23874187]

139. Zamft BM, Marblestone AH, Kording K, Schmidt D, Martin-Alarcon D, Tyo K, Boyden ES, Church G. Measuring cation dependent DNA polymerase fidelity landscapes by deep sequencing. PLoS One. 2012; 7:e43876. [PubMed: 22928047]

140. Hsieh CL, Pu Y, Grange R, Psaltis D. Digital phase conjugation of second harmonic radiation emitted by nanoparticles in turbid media. Opt Express. 2010; 18:12283–12290. [PubMed: 20588353]

141. Wang YM, Judkewitz B, DiMarzio CA, Yang CH. Deep-tissue focal fluorescence imaging with digitally time-reversed ultrasound-encoded light. Nat Commun. 2012:3.

142. Judkewitz B, Wang YM, Horstmeyer R, Mathy A, Yang CH. Speckle-scale focusing in the diffusive regime with time reversal of variance-encoded light (TROVE). Nat Photonics. 2013; 7:300–305. [PubMed: 23814605] •The authors propose TROVE as a method that overcomes the current limits on ultrasound resolution in TRUE. By shining several random wavefronts onto the scattering sample, measuring the output optical fields, and then statistically computing the combination of wave fields whose total energy equals that of the desired speckle grain, they can focus ultrasonically frequency-shifted light inside a scattering medium onto spots as small as an optical speckle grain. Although only validated *ex vivo*, this method can pave the way towards minimally-invasive light delivery and collection deeply in living tissue.

143. Jang M, Ruan H, Vellekoop IM, Judkewitz B, Chung E, Yang C. Relation between speckle decorrelation and optical phase conjugation (OPC)-based turbidity suppression through dynamic scattering media: a study on in vivo mouse skin. Biomed Opt Express. 2015; 6:72–85. [PubMed: 25657876]

144. Wen X, Jacques SL, Tuchin VV, Zhu D. Enhanced optical clearing of skin in vivo and optical coherence tomography in-depth imaging. J Biomed Opt. 2012; 17:066022. [PubMed: 22734778]

145. Genina EA, Bashkatov AN, Kolesnikova EA, Basko MV, Terentyuk GS, Tuchin VV. Optical coherence tomography monitoring of enhanced skin optical clearing in rats in vivo. J Biomed Opt. 2014; 19:21109. [PubMed: 24105426]

146. Connell BJ, Lortat-Jacob H. Human immunodeficiency virus and heparan sulfate: from attachment to entry inhibition. Front Immunol. 2013; 4:385. [PubMed: 24312095]

147. Jones CT, Catanese MT, Law LMJ, Khetani SR, Syder AJ, Ploss A, Oh TS, Schoggins JW, MacDonald MR, Bhatia SN, et al. Real-time imaging of hepatitis C virus infection using a fluorescent cell-based reporter system. Nat Biotechnol. 2010; 28:167–171. [PubMed: 20118917]

148. Sattentau Q. Avoiding the void: cell-to-cell spread of human viruses. Nat Rev Microbiol. 2008; 6:815–826. [PubMed: 18923409]

149. Wu Z, Asokan A, Samulski RJ. Adeno-associated virus serotypes: vector toolkit for human gene therapy. Mol Ther. 2006; 14:316–327. [PubMed: 16824801]

150. Fiege JK, Langlois RA. Investigating Influenza A Virus Infection: Tools To Track Infection and Limit Tropism. J Virol. 2015; 89:6167–6170. [PubMed: 25855737]
151. Kollarik M, Carr MJ, Ru F, Ring CJ, Hart VJ, Murdock P, Myers AC, Muroi Y, Undem BJ. Transgene expression and effective gene silencing in vagal afferent neurons in vivo using recombinant adeno-associated virus vectors. J Physiol. 2010; 588:4303–4315. [PubMed: 20736420]
152. Zhang H, Yang B, Mu X, Ahmed SS, Su Q, He R, Wang H, Mueller C, Sena-Esteves M, Brown R, et al. Several rAAV vectors efficiently cross the blood-brain barrier and transduce neurons and astrocytes in the neonatal mouse central nervous system. Mol Ther. 2011; 19:1440–1448. [PubMed: 21610699]
153. Ott HC, Matthiesen TS, Goh S-K, Black LD, Kren SM, Netoff TI, Taylor DA. Perfusion-decellularized matrix: using nature's platform to engineer a bioartificial heart. Nat Med. 2008; 14:213–221. [PubMed: 18193059]
154. Bianco P, Riminucci M, Gronthos S, Robey PG. Bone marrow stromal stem cells: nature, biology, and potential applications. Stem Cells. 2001; 19:180–192. [PubMed: 11359943]
155. Morrison SJ, Scadden DT. The bone marrow niche for haematopoietic stem cells. Nature. 2014; 505:327–334. [PubMed: 24429631]
156. Sugiyama T, Kohara H, Noda M, Nagasawa T. Maintenance of the Hematopoietic Stem Cell Pool by CXCL12-CXCR4 Chemokine Signaling in Bone Marrow Stromal Cell Niches. Immunity. 2006; 25:977–988. [PubMed: 17174120]
157. Wilson A, Trumpp A. Bone-marrow haematopoietic-stem-cell niches. Nat Rev Immunol. 2006; 6:93–106. [PubMed: 16491134]
158. Omatsu Y, Seike M, Sugiyama T, Kume T, Nagasawa T. Foxc1 is a critical regulator of haematopoietic stem/progenitor cell niche formation. Nature. 2014; 508:536–540. [PubMed: 24590069]
159. Mendez-Ferrer S, Michurina TV, Ferraro F, Mazloom AR, Macarthur BD, Lira SA, Scadden DT, Ma'ayan A, Enikolopov GN, Frenette PS. Mesenchymal and haematopoietic stem cells form a unique bone marrow niche. Nature. 2010; 466:829–834. [PubMed: 20703299]
160. Greenbaum A, Hsu YM, Day RB, Schuettpelz LG, Christopher MJ, Borgerding JN, Nagasawa T, Link DC. CXCL12 in early mesenchymal progenitors is required for haematopoietic stem-cell maintenance. Nature. 2013; 495:227–230. [PubMed: 23434756]
161. Hanoun M, Maryanovich M, Arnal-Estape A, Frenette PS. Neural Regulation of Hematopoiesis, Inflammation, and Cancer. Neuron. 2015; 86:360–373. [PubMed: 25905810]
162. Vakoc BJ, Lanning RM, Tyrrell JA, Padera TP, Bartlett LA, Stylianopoulos T, Munn LL, Tearney GJ, Fukumura D, Jain RK, et al. Three-dimensional microscopy of the tumor microenvironment in vivo using optical frequency domain imaging. Nat Med. 2009; 15:1219–1223. [PubMed: 19749772]
163. Magnon C, Hall SJ, Lin J, Xue X, Gerber L, Freedland SJ, Frenette PS. Autonomic nerve development contributes to prostate cancer progression. Science. 2013:341.
164. Colomba A, Ridley AJ. Analyzing the roles of Rho GTPases in cancer cell migration with a live cell imaging 3D–morphology-based assay. Methods Mol Biol. 2014; 1120:327–337. [PubMed: 24470035]
165. Fukamachi K, Ishida T, Usami S, Takeda M, Watanabe M, Sasano H, Ohuchi N. Total-circumference intraoperative frozen section analysis reduces margin-positive rate in breast-conservation surgery. Jpn J Clin Oncol. 2010; 40:513–520. [PubMed: 20189973]
166. Kasthuri N, Lichtman JW. Neurocartography. Neuropsychopharmacology. 2010; 35:342–343. [PubMed: 20010709]
167. Louveau A, Smirnov I, Keyes TJ, Eccles JD, Rouhani SJ, Peske JD, Derecki NC, Castle D, Mandell JW, Lee KS, et al. Structural and functional features of central nervous system lymphatic vessels. Nature. 2015; 523:337–341. [PubMed: 26030524]
168. Goodell MA, Nguyen H, Shroyer N. Somatic stem cell heterogeneity: diversity in the blood, skin and intestinal stem cell compartments. Nat Rev Mol Cell Biol. 2015; 16:299–309. [PubMed: 25907613]

169. Ross JD, Cullen DK, Harris JP, LaPlaca MC, DeWeerth SP. A three-dimensional image processing program for accurate, rapid, and semi-automated segmentation of neuronal somata with dense neurite outgrowth. Front Neuroanat. 2015; 9

170. Snippert HJ, van der Flier LG, Sato T, van Es JH, van den Born M, Kroon-Veenboer C, Barker N, Klein AM, van Rheenen J, Simons BD, et al. Intestinal crypt homeostasis results from neutral competition between symmetrically dividing Lgr5 stem cells. Cell. 2010; 143:134–144. [PubMed: 20887898]

171. Loulier K, Barry R, Mahou P, Le Franc Y, Supatto W, Matho KS, Ieng S, Fouquet S, Dupin E, Benosman R, et al. Multiplex cell and lineage tracking with combinatorial labels. Neuron. 2014; 81:505–520. [PubMed: 24507188]

172. Sharp FR, Liu JL, Bernabeu R. Neurogenesis following brain ischemia. Brain Res Dev Brain Res. 2002; 134:23–30. [PubMed: 11947934]

173. Nakatomi H, Kuriu T, Okabe S, Yamamoto S, Hatano O, Kawahara N, Tamura A, Kirino T, Nakafuku M. Regeneration of hippocampal pyramidal neurons after ischemic brain injury by recruitment of endogenous neural progenitors. Cell. 2002; 110:429–441. [PubMed: 12202033]

174. Gibson EM, Purger D, Mount CW, Goldstein AK, Lin GL, Wood LS, Inema I, Miller SE, Bieri G, Zuchero JB, et al. Neuronal Activity Promotes Oligodendrogenesis and Adaptive Myelination in the Mammalian Brain. Science. 2014

175. Bartzokis G, Lu PH, Heydari P, Couvrette A, Lee GJ, Kalashyan G, Freeman F, Grinstead JW, Villablanca P, Finn JP, et al. Multimodal Magnetic Resonance Imaging Assessment of White Matter Aging Trajectories Over the Lifespan of Healthy Individuals. Biol Psychiatry. 2012; 72:1026–1034. [PubMed: 23017471]

176. Taupin P, Gage FH. Adult neurogenesis and neural stem cells of the central nervous system in mammals. J Neurosci Res. 2002; 69:745–749. [PubMed: 12205667]

177. Hsiao EY, Patterson PH. Placental regulation of maternal-fetal interactions and brain development. Dev Neurobiol. 2012; 72:1317–1326. [PubMed: 22753006]

178. Hsiao EY, McBride SW, Chow J, Mazmanian SK, Patterson PH. Modeling an autism risk factor in mice leads to permanent immune dysregulation. Proc Natl Acad Sci U S A. 2012; 109:12776–12781. [PubMed: 22802640]

179. Hsiao EY, Patterson PH. Activation of the maternal immune system induces endocrine changes in the placenta via IL-6. Brain Behav Immun. 2011; 25:604–615. [PubMed: 21195166]

180. Kaya F, Mannioui A, Chesneau A, Sekizar S, Maillard E, Ballagny C, Houel-Renault L, DuPasquier D, Bronchain O, Holtzmann I, et al. Live Imaging of Targeted Cell Ablation in Xenopus: A New Model to Study Demyelination and Repair. J Neurosci. 2012; 32:12885–12895. [PubMed: 22973012]

181. Tapia JC, Kasthuri N, Hayworth KJ, Schalek R, Lichtman JW, Smith SJ, Buchanan J. High-contrast en bloc staining of neuronal tissue for field emission scanning electron microscopy. Nat Protoc. 2012; 7:193–206. [PubMed: 22240582]

182. Micheva KD, Smith SJ. Array tomography: a new tool for imaging the molecular architecture and ultrastructure of neural circuits. Neuron. 2007; 55:25–36. [PubMed: 17610815]

183. George MS, Sackeim HA, Rush AJ, Marangell LB, Nahas Z, Husain MM, Lisanby S, Burt T, Goldman J, Ballenger JC. Vagus nerve stimulation: a new tool for brain research and therapy. Biol Psychiatry. 2000; 47:287–295. [PubMed: 10686263]

184. Berthoud H-R, Neuhuber WL. Functional and chemical anatomy of the afferent vagal system. Autonomic Neuroscience. 2000; 85:1–17. [PubMed: 11189015]

185. Birmingham K, Gradinaru V, Anikeeva P, Grill WM, Pikov V, McLaughlin B, Pasricha P, Weber D, Ludwig K, Famm K. Bioelectronic medicines: a research roadmap. Nat Rev Drug Discov. 2014; 13:399–400. [PubMed: 24875080]

186. Alitalo K. The lymphatic vasculature in disease. Nat Med. 2011; 17:1371–1380. [PubMed: 22064427]

187. Bajénoff M, Egen JG, Koo LY, Laugier Jean P, Brau F, Glaichenhaus N, Germain RN. Stromal cell networks regulate lymphocyte entry, migration, and territoriality in lymph nodes. Immunity. 2006; 25:989–1001. [PubMed: 17112751]

188. Bulantová J, Macháček T, Panská L, Krejčí F, Karch J, Jährling N, Saghafi S, Dodt H-U, Horák P. Trichobilharzia regenti (Schistosomatidae): 3D imaging techniques in characterization of larval migration through the CNS of vertebrates. Micron. 2016; 83:62–71. [PubMed: 26897588]
189. Singh PK, Schaefer AL, Parsek MR, Moninger TO, Welsh MJ, Greenberg EP. Quorum-sensing signals indicate that cystic fibrosis lungs are infected with bacterial biofilms. Nature. 2000; 407:762–764. [PubMed: 11048725]
190. Ernst RK, Yi EC, Guo L, Lim KB, Burns JL, Hackett M, Miller SI. Specific Lipopolysaccharide Found in Cystic Fibrosis Airway Pseudomonas aeruginosa. Science. 1999; 286:1561–1565. [PubMed: 10567263]
191. Ramsey DM, Wozniak DJ. Understanding the control of Pseudomonas aeruginosa alginate synthesis and the prospects for management of chronic infections in cystic fibrosis. Mol Microbiol. 2005; 56:309–322. [PubMed: 15813726]
192. Tan SY, Chew SC, Tan SY, Givskov M, Yang L. Emerging frontiers in detection and control of bacterial biofilms. Curr Opin Biotechnol. 2014; 26:1–6. [PubMed: 24679251]
193. Hsiao EY, McBride SW, Hsien S, Sharon G, Hyde ER, McCue T, Codelli JA, Chow J, Reisman SE, Petrosino JF, et al. Microbiota modulate behavioral and physiological abnormalities associated with neurodevelopmental disorders. Cell. 2013; 155:1451–1463. [PubMed: 24315484]
194. Huang D, Swanson EA, Lin CP, Schuman JS, Stinson WG, Chang W, Hee MR, Flotte T, Gregory K, Puliafito CA, et al. Optical coherence tomography. Science. 1991; 254:1178–1181. [PubMed: 1957169]
195. Fujimoto JG, Brezinski ME, Tearney GJ, Boppart SA, Bouma B, Hee MR, Southern JF, Swanson EA. Optical biopsy and imaging using optical coherence tomography. Nat Med. 1995; 1:970–972. [PubMed: 7585229]
196. Schmitt JM, Knuttel A, Yadlowsky M, Eckhaus MA. Optical-coherence tomography of a dense tissue: statistics of attenuation and backscattering. Phys Med Biol. 1994; 39:1705–1720. [PubMed: 15551540]
197. Andersen PE, Thrane L, Yura HT, Tycho A, Jorgensen TM, Frosz MH. Advanced modelling of optical coherence tomography systems. Phys Med Biol. 2004; 49:1307–1327. [PubMed: 15128207]
198. Kruger RA, Liu P, Fang YR, Appledorn CR. Photoacoustic ultrasound (PAUS)--reconstruction tomography. Med Phys. 1995; 22:1605–1609. [PubMed: 8551984]
199. Fan Y, Mandelis A, Spirou G, Vitkin IA. Development of a laser photothermoacoustic frequency-swept system for subsurface imaging: theory and experiment. J Acoust Soc Am. 2004; 116:3523–3533. [PubMed: 15658704]
200. Wang LV. Multiscale photoacoustic microscopy and computed tomography. Nat Photonics. 2009; 3:503–509. [PubMed: 20161535]
201. Wang LV, Hu S. Photoacoustic tomography: in vivo imaging from organelles to organs. Science. 2012; 335:1458–1462. [PubMed: 22442475]
202. Fujimoto JG. Optical coherence tomography for ultrahigh resolution in vivo imaging. Nat Biotechnol. 2003; 21:1361–1367. [PubMed: 14595364]
203. Merali Z. Optics: Super vision. Nature. 2015; 518:158–160. [PubMed: 25673396]
204. Zhang EZ, Povazay B, Laufer J, Alex A, Hofer B, Pedley B, Glittenberg C, Treeby B, Cox B, Beard P, et al. Multimodal photoacoustic and optical coherence tomography scanner using an all optical detection scheme for 3D morphological skin imaging. Biomed Opt Express. 2011; 2:2202–2215. [PubMed: 21833358]
205. Beziere N, Lozano N, Nunes A, Salichs J, Queiros D, Kostarelos K, Ntziachristos V. Dynamic imaging of PEGylated indocyanine green (ICG) liposomes within the tumor microenvironment using multi-spectral optoacoustic tomography (MSOT). Biomaterials. 2015; 37:415–424. [PubMed: 25453969]
206. Ertürk A, Lafkas D, Chalouni C. Imaging Cleared Intact Biological Systems at a Cellular Level by 3DISCO. J. Vis. Exp. 2014 •A detailed video on conducting 3DISCO-based tissue clearing, which provides an informative, user-friendly follow-up to the *Nature Protocol* on the 3DISCO clearing technique.

207. Chen F, Tillberg PW, Boyden ES. Optical imaging Expansion microscopy. Science. 2015; 347:543–548. [PubMed: 25592419]

208. Murray E, Cho JH, Goodwin D, Ku T, Swaney J, Kim SY, Choi H, Park YG, Park JY, Hubbert A, et al. Simple, Scalable Proteomic Imaging for High-Dimensional Profiling of Intact Systems. Cell. 2015; 163:1500–1514. [PubMed: 26638076]

209. Bucher D, Scholz M, Stetter M, Obermayer K, Pflüger HJ. TCorrection methods for three-dimensional reconstructions from confocal images: I issue shrinking and axial scaling. J Neurosci Methods. 2000; 100:135–143. [PubMed: 11040376]

Box 1. Glossary of acronyms and terminology related to tissue-clearing and cell-mapping

3DISCO: Three-Dimensional Imaging of Solvent-Cleared Organs; 3DISCO and uDISCO versions.
AAV: Adeno-Associated Virus; multiple natural and non-natural serotypes, including AAV-PHP.B.
BABB: Benzyl Alcohol and Benzyl Benzoate; BABB and Murray's Clear techniques.
Brainbow: stochastic expression of multiple fluorescent proteins from a single transgene; Brainbow v1.0–3.2 in addition to other variants (e.g., Autobow, Flybow, Zebrabow, R26R–Confetti, MAGIC Marker).
CaMPARI: Calcium-Modulated PhotoActivatable Ratiometric Integrator of neuronal activity
CLARITY: Clear Lipid-exchanged Acrylamide-hybridized Rigid Imaging/immunostaining/*in situ* hybridization-compatible Tissue hYdrogel; CLARITY, advanced CLARITY, passive CLARITY, and stochastic-electrotransport versions.
CREATE: Cre-recombination-based AAV Targeted Evolution
CUBIC: Clear Unobstructed Brain Imaging cocktails and Computational analysis; CUBIC, advanced CUBIC and perfusion-CB variations.
Clear: a formamide-based optical clearing method; ClearT and ClearT2 (formamide/polyethylene glycol) variation.
DMSO: dimethyl sulfoxide
EDTA:ethylenediaminetetraacetic acid
ETC: Electrophoretic Tissue Clearing; clearing approach of CLARITY.
ePACT: expansion-PACT
ExM: Expansion Microscopy
Fruit: optical clearing method that utilizes an aqueous cocktail of fructose, urea, and α-thioglycerol.
GRASP: *GFP Reconstitution Across Synaptic Partners*
HCR: Hybridization Chain Reaction; operable with RNA and DNA probes
iDISCO: Immunolabeling-enabled 3D Imaging of Solvent-Cleared Organs; iDISCO and iDISCO+ variation.
IHC: Immunohistochemistry
NPS: Neuronal Positioning System
PACT: PAssive Clarity Technique
PACT-deCAL: PACT-deCALcification
PARS: Perfusion-assisted Agent Release *in Situ* ; PARS and PARS-CSF variation.
PFA: Paraformaldehyde
RI: refractive index
RIMS: Refractive Index Matching Solution; RIMS (histodenz-based) and sRIMS (sorbitol-based) variation.
Sca*l*e: a urea-based optical clearing method; Sca*l*eA2 and Sca*l*eU2 versions.
Sca*l*eS: a sorbitol-based optical clearing method; includes AbSca*l*e, Chemsca*l*e, and Sca*l*eSQ variations.
SDS: sodium dodecyl sulfate
SeeDB: See Deep Brain; SeeDB, SeeDB37 and SeeDB37ht variations.
smFISH: single-molecule Fluorescence *In Situ* Hybridization
Spalteholz's preparation: Benzyl benzoate and methyl salicylate
SWITCH: System-*W*de control of Interaction *T*ime and kinetics of CHemicals
TDE: 2,2'-thiodiethanol
Tissue-Hydrogel: tissue structure and/or molecular content may be stabilized via tissue-hydrogel crosslinking or embedding; multiple hydrogel

formulations, including any/all of acrylamide, bisacrylamide, paraformaldehyde, glutaraldehyde, sodium acrylate, agarose.
TRAP: *T*argeted *R*ecombination in *A*ctive *P*opulations
TRIO: ‘Tracing the Relationship between Input and Output’ method; TRIO and cTRIO methods.
TRUE: Time-Reversal Ultrasound-Encoded

Highlights

1. Tissue clearing and viral vectors for resolved 3D imaging of unsevered circuits
2. Size-adjustable tissue-hydrogels for sample stabilization and selective extraction
3. Whole-body clearing and labeling via *P*erfusion-assisted *A*gent *R*elease in *S*itu
4. High-throughput method for in vivo vector selection and bodywide transduction mapping
5. AVV vector for transgene expression brainwide via systemic injection in the adult

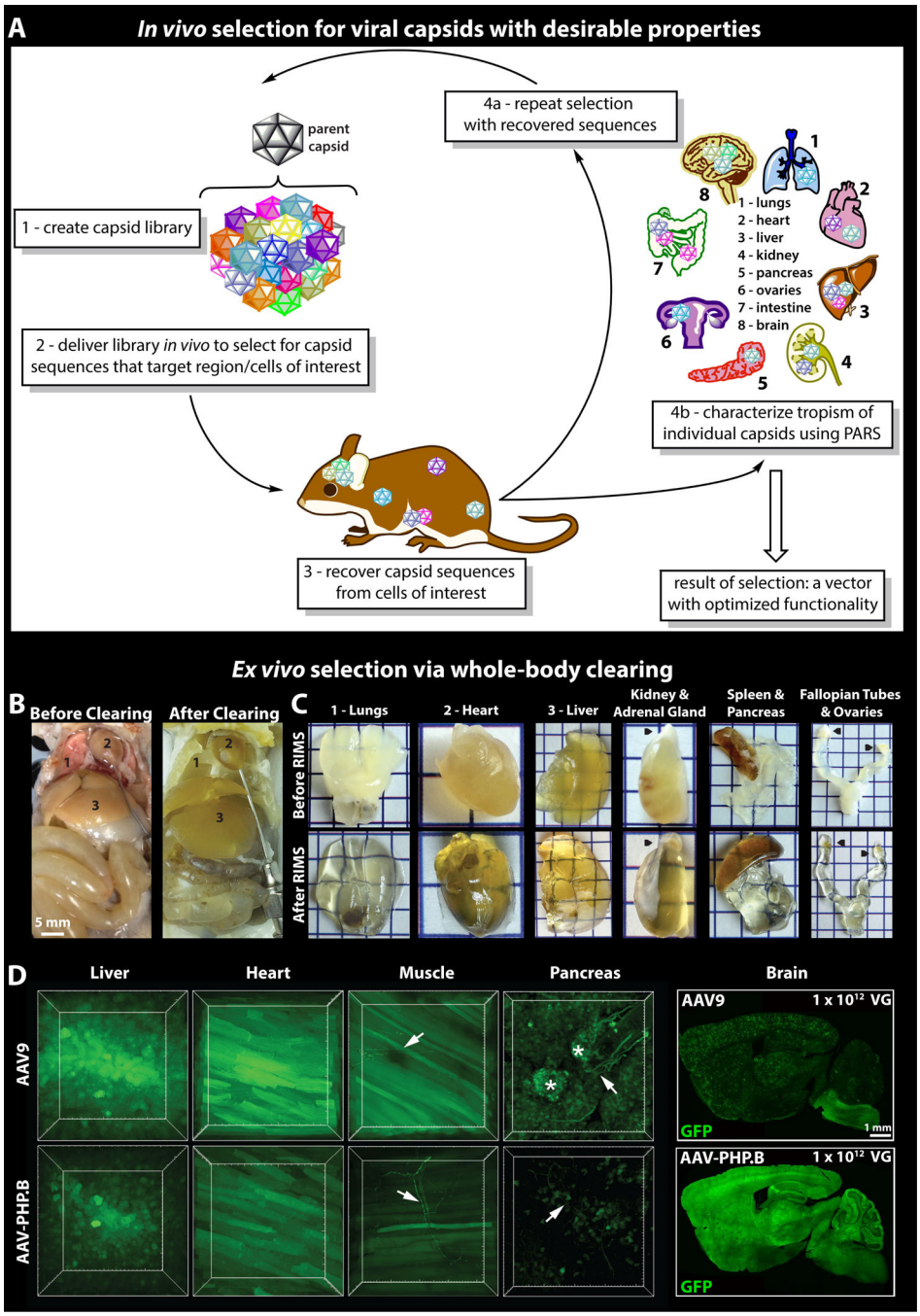

Figure 1.

Concept for an *in vivo* selection technology for panning large-scale libraries to identify compounds or biologicals with optimized physiological properties. Whole-body tissue clearing can then facilitate biodistribution mapping. For example, to engineer viral vectors for more effective transgene delivery, one strategy involves exposing live cells or whole-organisms to AAV capsid libraries and then identifying positive hits via a cell or tissue type-dependent recovery strategy (**A**). Whole-body clearing by Perfusion-Assisted Agent Release in Situ (PARS, [32,41]) speeds up the multi-organ assessment of vector variants expression

profiles. Internal organs before and after clearing (**B**). Individual PARS-cleared organs (**C**) before (top) or after (bottom) equilibration in RIMS, a Refractive Index Matching Solution [32,41], as imaging media. Black pointers correspond to the adrenal gland on the kidney, and to the ovaries on the fallopian tubes. Each square represents 0.5 cm^2. The qualitative assessment of cell-type transduction can be conducted by packaging fluorescent reporters in individual capsid variants and then simultaneously clearing all organs *in situ* (**D**). As proof-of-principle, a novel capsid variant (AAV-PHP.B, bottom), selected for enhanced brain transduction, was rapidly evolved from AAV9 (top). Comparisons of PARS-cleared organs demonstrate that AAV-PHP.B and AAV9 have similar cellular tropisms outside of the brain. Arrows (→) indicate neuronal morphology, and asterisks (*) designate pancreatic islets. Differences in brain transduction are depicted in the images of mouse brain sagittal sections. Figures 2A and 2D adapted from [53], and figures 2B–C adapted from [41].

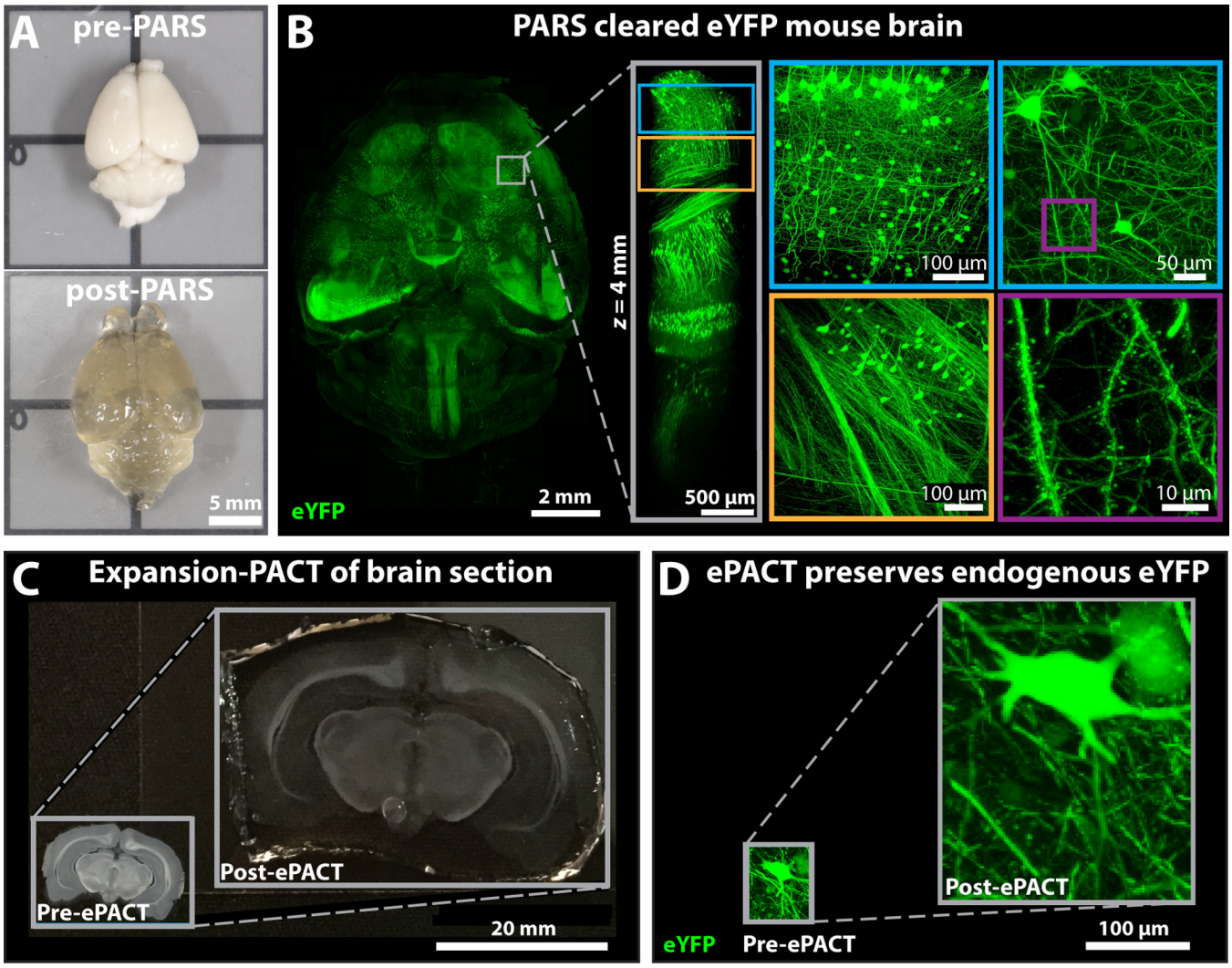

Figure 2.

Clearing techniques that enable high-resolution, volumetric imaging of tissue architecture and cellular morphology. Whole-body hydrogel embedding and detergent-based clearing via the PARS-CLARITY method [22,32,37,41] preserves gross tissue structure (**A**) and fine neuronal processes (**B**) alike, while the purposeful expansion of these tissue-hydrogel hybrids via water absorption (**C**) allows the visualization of subcellular detail via either native fluorescence (**D**), or probes for protein and nucleic acid detection [32]. ePACT permits the clearing and 4-fold expansion of 100 µm thick coronal brain sections with preservation of tissue shape, cellular morphology and native fluorescence. Figures 1A–B adapted from [32], and figures 1C–D adapted from [41].

Table 1

Anticipated Biomedical Applications of Modern Clearing Techniques

Application Areas	Cleared Tissue and Complementary Technologies
Assessing biodistribution of chemicals or biologicals; and screening compound libraries [53,91,146–152]	**Whole-body clearing[a] of rodents (embryos through aged adult; see Figure 1) Excised whole-organ delipidation through major blood vessels in larger mammalian subjects (e.g. pigs, non-human primates) [101,153] CREATE platform for viral vector screening in cleared samples (Fig. 1) [53]**
Labeling and imaging through dense, complex tissues [154–161] Mapping discrete cellular niches (e.g. stem cells, tumors) [162–168]	**PACT-deCAL [41], BABB [27,106] for bone Clearing tissue biopsies[b] and excised organs, or whole-body perfusion-clearing[a] in cancer models**
3D–tracing long-range fiber bundles (e.g. vagus nerve); lineage-mapping in neurodevelopment [169]	**Viral or transgenic labeling technologies (e.g. Brainbow [7], TRIO [6], Confetti [170], MAGIC markers [171]; Box 1) followed by whole-body clearing**
Monitoring the progression of cell death and tissue damage (e.g. stroke, infarcts), and the corresponding re-oxygenation [172,173]	**Whole-organ or whole-body clearing Perfusion labelling to counterstain intact vasculature and surrounding tissues**
Tracking nerve/axon regeneration and de/re-myelination; examining neuroplasticity at the synaptic level [28,115,174–180]	**Whole-body perfusion-clearing[a] and perfusion-labelling, and PACT-deCAL [41] to clear the vertebral column Co-registration of array tomography [181,182], light and electron microscopy datasets [8,73,161,183–187]**
Spectrally resolving subcellular labels (e.g. single molecule transcripts) within native tissue	**Multiplexed labelling and/or sequential barcoding with FISH [120–122] and HCR [127,128]; Neuronal positioning system (NPS) [8] Hydrogel-embedding and expansion-clearing (ExM [72], ePACT [41])**
Exploring topics in parasitology [188] and microbiology (e.g., biofilm formation, microbe distribution within a niche [189–192], host interaction with the microbiome [64,193])	**Hydrogel-embedding of fragile samples'[b], followed by gentle, passive whole-organ clearing to maintain bacterial colonization**
Extending the imaging depth range and resolution for optical coherence tomography [194–197] and photoacoustic tomography [141–143,145,198–205]	**Future prospects for optically clearing living tissue with optical and/or contrast clearing reagents (e.g. varying ratios of PEG-400, DMSO, and/or glycerol)**

[a]For whole-body clearing and perfusion-labeling methods, see [31,32,39,41], with detailed methods on PARS and perfusion-CUBIC in their respective *Nature Protocols*

[b]For further advice, see troubleshooting instructions at http://www.nature.com/nprot/journal/v10/n11/fig_tab/nprot.2015.122_T5.html [41]

Table 2

Methodological comparison and important considerations when choosing a tissue clearing protocol that achieves both macromolecular extraction and optical clarity.

Motivation	Method *Variations*	Sample Preparation[a]	Clearing Reagents[b]	Size Fluctuations	Fluorescence[c]	IHC[d]
Dehydration and Lipid Solvation						
To achieve transparency rapidly using organic solvents of high RI (precursors: Spalteholz [55], BABB [27])	**3DISCO [26,28,38,206]**	tetrahydrofuran dehydration	dichloromethane lipid solvation	shrinkage	YES (1–4d)	Limited
	iDISCO [36]	methanol dehydration or DMSO, PBS	dichloromethane	shrinkage	YES (1–4d)	YES
	uDISCO[e]	n/p[f]	n/p	shrinkage	YES	YES
Partial delipidation and hyperhydration						
To obtain a fluorescence-compatible solvent alternative via hyper-hydration of the delipidized sample	**Sca/eA2-U2 [23]**	n/a[f]	4 M urea, 10–30% glycerol hyperhydration	expansion	YES	NO
	Sca/eS (*AbSca/e, ChemSca/e Sca/eSQ*) [40]	n/a	2.7–9.1 M urea, 20–40% sorbitol, ≤5.0% Triton X-100, DMSO	NO	YES	YES
	CUBIC [25], *with decolorization* [35,39]	n/a	25% urea-50% sucrose aminoalcohol decolorization 15% Triton X-100 delipidation	expansion	YES	YES
Targeted biomolecule retention and rigorous delipidation						
To stabilize sample structure, macromolecular content, and fluorescent labeling using size adjustable, tissue-binding hydrogels	**CLARITY [22,37,62,110]**	tissue-hydrogel	4% SDS ETC delipidation [f]	reversible expansion	YES	YES
	CLARITY variations [29,30,110]		4% SDS ETC 4% SDS diffusion		YES	YES
	Stochastic Electrotransport [81]		4% SDS stochastic ETC		YES	YES
	PARS [32,41] *PACT* [32,41]	tissue-hydrogel	8% SDS perfusion 8% SDS diffusion	reversible expansion	YES	YES
	PACT-deCAL	tissue-hydrogel	8% SDS diffusion EDTA/EGTA decalcification	NO	YES	YES

Motivation	Method *Variations*	Sample Preparation[a]	Clearing Reagents[b]	Size Fluctuations	Fluorescence[c]	IHC[d]
	ExM [207] *ePACT* [41]	superabsorbent hydrogel	enzymatic digestion ±clearing	4–5x expansion	YES	YES
	SWITCH [208]	glutaraldehyde-tissue gel	200mM SDS diffusion, 60–80 °C	NO	NO	YES
Whole-body perfusion clearing						
To preserve body-brain connections and accelerate adult whole-organ preparation via clearing *in situ*	**PARS**	tissue-hydrogel	8% SDS perfusion clearing	minimal expansion	YES	YES-perfusion
	Perfusion CUBIC [39]	tissue-hydrogel	CUBIC reagent perfusion	n/d[f]	YES	Limited-perfusion
	Perfusion FRUIT [31]	n/a	FRUIT reagent perfusion	n/d	n/d	NO

[a] Sample preparation aside from standard fixation and brief post-fixation (e.g. transcardial perfusion with 4% PFA).

[b] Chemically/mechanically removing tissue macromolecular components (e.g. lipids, heme) to improve light probe penetration and reduce light scattering.

[c] Fluorescence preservation varies with fluorophore and user technique. A binary classification: YES = overall preservation of endogenous fluorescence, with any signal dimming mild; NO = major or complete endogenous fluorescence quenching due to reagent or procedural incompatibility with common fluorophores; if rapid signal decay, timeline for imaging in "( )". Also of note, moderate loss of fluorescence in CUBIC, PACT, and SeeDB tissues, and major quenching in 3DISCO tissues has been reported elsewhere [40].

[d] YES, NO: Compatible, incompatible with IHC and fluorescent labeling in thick samples and with multiple fluorophores; Limited: IHC possible with small-molecule stains and some antibodies, restrictions in immunofluorescence and/or deep antibody penetration; Perfusion-delivery of IHC reagents noted where applicable.

[e] Personal communication with Dr. Ali Ertürk on uDISCO, which allows preservation of endogenous fluorescence in fine processes for several weeks to months.

[f] abbreviations: n/p = not published, n/d = not determined, n/a = not applicable; see Box 1 for complete list.

Table 3

Sample mounting for enhanced optical clarity.

Method[a]	Sample Preparation	Clearing Reagents	Size Fluctuations	Fluorescence
organic solvents RI ~ 1.52–1.57	none	methyl salicylate [209]	shrinkage	NO
	Ultramicroscopy [27]	BABB	shrinkage	Y/N»
	3DISCO iDISCO	dibenzyl ether	shrinkage	Y/N
amides RI ~ 1.38–1.44	ClearT, ClearT2 [24]	formamide ± PEG	none, n/d[b]	Y/N
	Sca/eA2, Sca/eS, CUBIC, FRUIT	urea	slight -moderate expansion	YES
polyol and concentrated sugar or sugar alcohol solutions RI ~ 1.43–1.50, tunable	CLARITY, PACT, PARS	glycerol	slight expansion	YES
	SeeDB [21,102]	fructose	minimal	YES
	FRUIT	fructose + thioglycerol + urea	slight expansion	YES
	Sca/eA2	glycerol + urea	moderate expansion	YES
	CUBIC	sucrose + urea + triethanolamine	moderate expansion	YES
	Sca/eS, PARS, PACT	sorbitol, sRIMS	slight - moderate expansion	YES
aqueous contrast media RI ~ 1.46, tunable	CLARITY	Focus Clear: Diatrizoic acid	slight expansion	YES
	PACT, PARS, RIMS	RIMS: Histodenz	acute shrinkage, gradual expansion	YES
aqueous mounting media RI ~ 1.33–1.52, tunable	TDE [34]	2,2'-thiodiefhanol [83]	none	YES

[a] Optical clarity, or reduced light scattering through tissue, may be enhanced via homogenizing the refractive indices throughout heterogeneous tissues and at all material interfaces between the sample and objective lens

[b] Y/N = signal decay may necessitate prompt imaging upon sample mounting